

GaN-based two-dimensional surface-emitting photonic crystal lasers with AlN/GaN distributed Bragg reflector

Tien-Chang Lu,^{a)} Shih-Wei Chen, Li-Fan Lin, Tsung-Ting Kao, Chih-Chiang Kao, Peichen Yu, Hao-Chung Kuo, and Shing-Chung Wang
Department of Photonics and Institute of Electro-Optical Engineering, National Chiao-Tung University, 1001 Ta Hsueh Rd., Hsinchu 30050, Taiwan

Shanhui Fan

Department of Electrical Engineering, Stanford University, Stanford, California 94305, USA

(Received 9 August 2007; accepted 14 December 2007; published online 11 January 2008)

GaN-based two-dimensional (2D) surface-emitting photonic crystal (PC) lasers with AlN/GaN distributed Bragg reflectors are fabricated and demonstrated. The lasing threshold energy density is about 3.5 mJ/cm^2 per pulse under optical pumping at room temperature. Only one dominant emission wavelength of 424.3 nm with a narrow linewidth of 1.1 \AA above the threshold is observed. The laser emission covers whole circularly 2D PC patterns ($50 \mu\text{m}$ in diameter) with a small divergence angle. The lasing wavelength emitted from 2D PC lasers with different lattice constants occurs at the calculated band-edges provided by the PC patterns. The characteristics of large area, small divergence angle, and single mode emission from the GaN-based 2D surface-emitting PC lasers should be promising in high power blue-violet emitter applications. © 2008 American Institute of Physics. [DOI: 10.1063/1.2831716]

Photonic crystals (PCs) have many advantages for controlling light emission and propagations, and have been the basis for various new optical devices.¹⁻³ Two kinds of semiconductor PC lasers have been developed. The first kind uses photonic crystal nanocavity, which has a high Q value and a small modal volume. Such nanocavity laser can achieve strong Purcell effect and low-threshold lasing.^{4,5} The second kind utilizes multidirectional distributed feedback effect near the band edges in two-dimensional (2D) PC structures. Such surface emitting lasers have potential to operate as a high-power source producing single-mode lasing over a broad area.^{6,7}

Most works on PC lasers have been done using organic, GaAs, and InP material systems that operate at longer wavelengths. Nitride-based materials have attracted a great attention in the early 1990s due to the large direct band gap and the promising potential for many optoelectronic devices.^{8,9} However, few GaN-based PC lasers that have been reported are all of a nanocavity type,¹⁰ which is different from what we will report here. In this letter, we demonstrate the fabrication and room temperature lasing action of GaN-based 2D surface-emitting PC structures with bottom AlN/GaN distributed Bragg reflector (DBR). For a $50 \mu\text{m}$ diameter PC pattern with hexagonal lattice and circle unit cell, the lasing threshold is 3.5 mJ/cm^2 . Above threshold, a single peak with wavelength at 424.3 nm and a linewidth of 1.1 \AA is observed. The laser emits from a broad emission area and the emitted beam has a small divergence angle. By varying the lattice constant of the PC pattern, different normalized lasing frequencies corresponding to different band edges are demonstrated.

The GaN-based 2D surface-emitting PC laser, shown schematically in Fig. 1(a), was grown by a metal-organic chemical vapor deposition system on c -face 2 in diameter sapphire. Trimethylindium, trimethylgallium, trimethylalu-

minum, and ammonia were used as the In, Ga, Al, and N sources, respectively. The 35 pairs quarter-wave GaN/AlN DBR grown on a $2 \mu\text{m}$ thick undoped GaN buffer layer was crack free and had a flat surface. The detailed growth parameters were reported elsewhere.¹¹ Then, an active region grown atop the DBR typically composed of ten $\text{In}_{0.2}\text{Ga}_{0.8}\text{N}$ quantum wells (QWs) ($L_W=2.5 \text{ nm}$) with GaN barriers ($L_B=7.5 \text{ nm}$), and was surrounded by a 560 nm thick Si-doped n -type GaN and a 200 nm thick Mg-doped p -type GaN layer.

The typical photoluminescence (PL) spectrum had a peak centered at a wavelength of 425 nm with a linewidth of 25 nm . At normal incidence at room temperature, the DBR

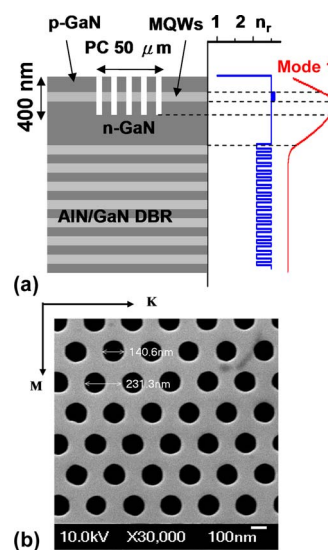


FIG. 1. (Color online) (a) Schematic layer structure of GaN-based 2D surface-emitting PC lasers with bottom AlN/GaN distributed Bragg reflector and the lowest order calculated mode intensity profile along with the refractive index distribution. (b) Top view scanning electron microscope images of the PC structures with hexagonal lattices and circle unit cells.

^{a)}Electronic mail: timclu@mail.nctu.edu.tw.

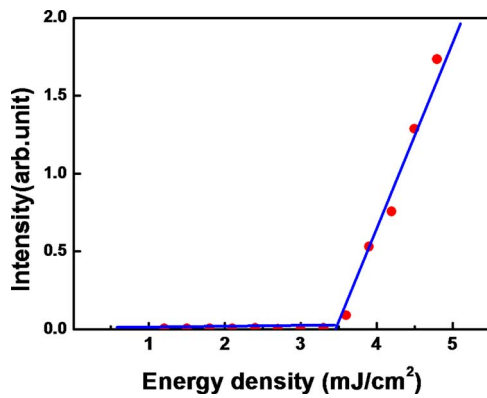


FIG. 2. (Color online) Measured output intensity versus input excitation energy density from the GaN-based 2D surface-emitting PC lasers with bottom AlN/GaN distributed Bragg reflectors at room temperature.

showed the highest reflectivity of 99% at the center wavelength of 430 nm, with a stopband width of about 30 nm, measured by an $n&k$ ultraviolet-visible spectrometer. The as-grown sample was then first deposited with a hard mask consisting of a SiN layer of 200 nm by plasma-enhanced chemical vapor deposition, followed by a soft mask consisting of a polymethylmethacrylate (PMMA) layer of 150 nm. Using electron-beam lithography, we defined on the soft mask a hexagonal PC pattern with the lattice constant a ranging from 190 to 300 nm and the circular hole diameter r chosen such that r/a is about 0.28. The whole PC pattern is of a circular shape with a diameter of 50 μm . Then, the PC pattern on soft mask was transferred to SiN film by inductively coupled plasma-reactive ion etching (ICP-RIE). After the PMMA layer was removed by acetone, we used ICP-RIE to etch down the as-grown sample to about 400 nm deep. The etching penetrated the QW active regions and created the PC patterns in the nitride layers. Finally, the SiN hard mask was removed by buffered oxide etch dipping. The top view of the hexagonal PC pattern on the GaN-based structure thus created was shown in Fig. 1(b).

The optical pumping was performed using a frequency-tripled Nd:YVO₄ 355 nm pulsed laser with a pulse width of ~ 0.5 ns at a repetition rate of 1 KHz. The pumping laser beam had a spot size of 50 μm and was normally incident onto the sample surface covering the whole PC pattern area. The light emission from the sample was collected by a 15 \times objective lens through a fiber with a 600 μm core, and coupled into a spectrometer with a charge-coupled device (CCD). The spectral resolution is about 0.1 nm for spectral output measurement.

Figure 2 demonstrates the output emission intensity as a function of the pumping energy density from the sample with PC lattice constant of 290 nm. The clear threshold characteristic was observed at the threshold pumping energy density of 3.5 mJ/cm², with a peak power density of 7 MW/cm². Then the laser output increases abruptly with the excitation energy density beyond the threshold. Figure 3 shows the excitation energy density dependent emission spectra. These spectra clearly show the transition behavior from spontaneous emission to stimulated emission with a single dominant peak. Above the threshold, we can observe only one dominant peak wavelength of 424.3 nm with a full width at half maximum (FWHM) of 0.11 nm limited by our measurement resolution.

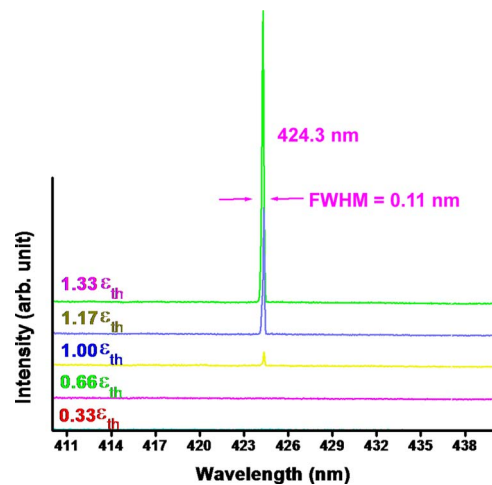


FIG. 3. (Color online) Emission spectra under varied excitation energy density from the GaN-based 2D surface-emitting PC lasers with bottom AlN/GaN distributed Bragg reflectors at room temperature.

It is worth noting that the single mode lasing phenomenon only occurs in the area with PC patterns. On the other hand, multiple lasing peaks were occurred when the area without PC patterns was pumped at the threshold energy density two order of magnitude higher. The normalized frequency (lattice constant over wavelength, a/λ) for the lasing wavelength emitted from our PC lasers with different lattice constants were plotted, as shown in Fig. 4(a). All the PC lasers have lasing peaks in a range from 401 to 425 nm. It can be seen that the normalized lasing frequency (dotted points in the figure) increased with the lattice constant in a discontinuous and steplike fashion. To calculate the band diagram of the hexagonal PC patterns in this structure, we employ the plane-wave expansion method in two-dimensions with an effective index approach that took into account the effects of partial modal overlap of electromagnetic fields with the PC structures.¹² As a starting point, the ratio of light confined within the 2D PC structure to light extended in the entire device Γ_g and the effective refractive index of the entire device n_{eff} were first estimated by the transfer matrix method. The calculation shows that the lowest order guided mode has the highest confinement factor for both PC and multiple quantum well regions, as shown in Fig. 1(a), and the Γ_g and n_{eff} are estimated to be 0.563 and 2.495, respectively. Then, we determine the effective dielectric constants of the two materials in the unit cell, ϵ_a and ϵ_b , using $n_{\text{eff}}^2 = f\epsilon_a + (1-f)\epsilon_b$ and $\Delta\epsilon = \epsilon_b - \epsilon_a = \Gamma_g(\epsilon_{\text{mat}} - \epsilon_{\text{air}})$, where, the $f = (2\pi r^2 / \sqrt{3}a^2)$ is a filling factor and ϵ_{mat} and ϵ_{air} are dielec-

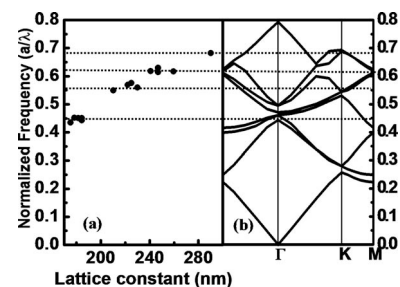


FIG. 4. (a) Normalized frequency as a function of the lattice constant. The solid circle points are the lasing wavelengths from the different PC structures. (b) Calculated band diagram of the 2D hexagonal-lattice structure. The dotted lines are guides for band edges.

tric constants of GaN ($\epsilon_a=2.5^2$) and air ($\epsilon_b=1^2$), respectively. The values of $\epsilon_a(4.11)$ and $\epsilon_b(7.07)$ thus obtained were then put into the calculation of the band diagram for the 2D hexagonal-lattice structure with $r/a=0.28$.

Figure 4(b) shows the calculated band diagram of the 2D hexagonal-lattice structure for transverse-electric mode. It can be expected that the lasing occurs at special points such as at Brillouin-zone boundary near the band edges, because the Bragg condition is satisfied and the density of states is higher in these points.¹² At these lasing points, wave can propagate in different directions and couple with each other. The dotted lines are guides for band edges calculated in Fig. 4(b) and extended horizontally to Fig. 4(a) with the same normalized frequency. It can be seen that different groups of the normalized frequency observed in the PC samples with different lattice constants occur exactly at band edges such as Γ , M , and K points, indicating that the laser operation was provided by multidirectional distributed feedback in the 2D PC structure.¹³ The characteristics of Γ , M , and K points lasing can be further identified by the polarization angle of the output emission.¹⁴ Note that the output intensity is higher when some of the lasing frequencies are in the stopband of DBR, which could be due to that the bottom DBR here could be treated as a high reflectivity reflector, facilitating top-emission efficiency.

The lasing area of the GaN-based 2D surface-emitting PC laser, obtained by a CCD camera is relatively large which covers almost whole area of PC pattern with only one dominant lasing wavelength. The measured FWHM of laser emission divergence angle is smaller than 5° , which is limited by our measurement setup, indicating that the surface emission is almost normal to the PC surface. It's interesting to note that the threshold power density of GaN-based 2D surface-emitting PC laser is in the same order of or even better than the threshold for GaN-based vertical-cavity surface emitting lasers (VCSELs) we demonstrated recently.¹⁵ Unlike the small emission spots observed in the GaN-based VCSELs, the large-area emission in 2D surface-emitting PC laser has great potential in applications required high power output operation.

In conclusion, the GaN-based 2D surface-emitting PC lasers with AlN/GaN bottom DBRs are fabricated. The laser action is achieved under the optical pumping at room tem-

perature with a threshold pumping energy density of about 3.5 mJ/cm^2 for the sample with PC lattice constant of 290 nm. The laser emits one dominant wavelength of 424.3 nm with a linewidth of about 1.1 \AA . All normalized frequency of investigated PC lasing wavelength can correspond to the calculated Brillouin-zone boundary provided by 2D hexagonal-lattice PC patterns. The emission images of the laser indicate that the stimulated emission occurs over a large area with a small divergence angle. The GaN-based 2D surface-emitting PC lasers with large area, small divergence angle and single mode emission should be very attractive in high power applications.

The authors would like to gratefully acknowledge A. E. Siegman at Stanford for his fruitful suggestion. The study was supported by the MOE ATU program and, in part, by the National Science Council in Taiwan under Contract Nos. NSC 95-2120-M-009-008, NSC 95-2752-E-009-007-PAE, and NSC 95-2221-E-009-282.

¹E. Yablonovitch, Phys. Rev. Lett. **58**, 2059 (1987).

²S. John, Phys. Rev. Lett. **58**, 2486 (1987).

³J. D. Joannopoulos, P. R. Villeneuve, and S. Fan, Nature (London) **386**, 143 (1997).

⁴O. Painter, R. K. Lee, A. Scherer, A. Yariv, J. D. O'Brien, P. D. Dapkus, and I. Kim, Science **284**, 1819 (1999).

⁵H. G. Park, S. H. Kim, S. H. Kwon, Y. G. Ju, J. K. Yang, J. H. Baek, S. B. Kim, and Y. H. Lee, Science **305**, 1444 (2005).

⁶M. Meier, A. Mekis, A. Dodabalapur, A. Timko, R. E. Slusher, J. D. Joannopoulos, and O. Nalamasu, Appl. Phys. Lett. **74**, 7 (1999).

⁷D. Ohnishi, T. Okano, M. Imada, and S. Node, Opt. Express **12**, 1562 (2004).

⁸S. Nakamura, M. Senoh, N. Iwasa, and S. Nagahama, Jpn. J. Appl. Phys., Part 2 **34**, L797 (1995).

⁹S. Nakamura, M. Senoh, S. Nagahama, N. Iwasa, T. Yamada, T. Matsushita, Y. Sugimoto, and H. Kiyoku, Appl. Phys. Lett. **70**, 868 (1997).

¹⁰C. F. Lai, P. Yu, T. C. Wang, H. C. Kuo, T. C. Lu, S. C. Wang, and C. K. Lee, Appl. Phys. Lett. **91**, 041101 (2007).

¹¹G. S. Huang, T. C. Lu, H. H. Yao, H. C. Kuo, S. C. Wang, C.-W. Lin, and Li Chang, Appl. Phys. Lett. **88**, 061904 (2006).

¹²M. Imada, A. Chutinan, S. Noda, and M. Mochizuki, Phys. Rev. B **65**, 195306 (2002).

¹³M. Notomia, H. Suzuki, and T. Tamamura, Appl. Phys. Lett. **78**, 1325 (2001).

¹⁴T. C. Lu, S. W. Chen, and T. T. Kao (unpublished).

¹⁵S. C. Wang, T. C. Lu, C. C. Kao, J. T. Chu, G. S. Huang, H. C. Kuo, S. W. Chen, T. T. Kao, J. R. Chen, and L. F. Lin, Jpn. J. Appl. Phys., Part 1 **46**, 5397 (2007).